



WNT11, a new gene associated with early onset osteoporosis, is required for osteoblastogenesis

Caroline Caetano da Silva ¹, Thomas Edouard ², Melanie Fradin³, Marion Aubert-Mucca², Manon Ricquebourg¹, Ratish Raman⁴, Jean Pierre Salles², Valérie Charon⁵, Pascal Guggenbuhl⁶, Marc Muller⁴, Martine Cohen-Solal¹ and Corinne Collet^{1,7,*}

¹INSERM U1132 and Université de Paris, Reference Centre for Rare Bone Diseases, Hospital Lariboisière, Paris F-75010, France

²Endocrine Bone Diseases and Genetics Unit, Reference Centre for Rare Diseases of Calcium and Phosphate Metabolism, ERN BOND, OSCAR Network, Pediatric Clinical Research Unit, Children's Hospital, RESTORE INSERM U1301, Toulouse University Hospital, Toulouse 31300, France

³Service de Génétique Clinique, Centre de Référence des Anomalies du Développement de l'Ouest, Hôpital Sud de Rennes, Rennes F-35033, France

⁴Laboratory for Organogenesis and Regeneration (LOR), GIGA-Research, Liège University, Liège 4000, Belgium

⁵Department of Radiology, CHU de Rennes, Rennes F-35000, France

⁶Department of Rheumatology, CHU de Rennes, Rennes F-35000, France

⁷Département de Génétique, UF de Génétique Moléculaire, Hôpital Robert Debré, APHP, Paris F-75019, France

*To whom correspondence should be addressed at: INSERM U1132, 2 rue Ambroise Paré, Paris 75010, France. Tel: +33 149956358; Fax: +33 149958452; Email: corinne.collet@aphp.fr

Abstract

Monogenic early onset osteoporosis (EOOP) is a rare disease defined by low bone mineral density (BMD) that results in increased risk of fracture in children and young adults. Although several causative genes have been identified, some of the EOOP causation remains unresolved. Whole-exome sequencing revealed a *de novo* heterozygous loss-of-function mutation in Wnt family member 11 (WNT11) (NM_004626.2:c.677_678dup p.Leu227Glyfs*22) in a 4-year-old boy with low BMD and fractures. We identified two heterozygous WNT11 missense variants (NM_004626.2:c.217G > A p.Ala73Thr) and (NM_004626.2:c.865G > A p.Val289Met) in a 51-year-old woman and in a 61-year-old woman, respectively, both with bone fragility. U2OS cells with heterozygous WNT11 mutation (NM_004626.2:c.690_721delfs*40) generated by CRISPR-Cas9 showed reduced cell proliferation (30%) and osteoblast differentiation (80%) as compared with wild-type U2OS cells. The expression of genes in the Wnt canonical and non-canonical pathways was inhibited in these mutant cells, but recombinant WNT11 treatment rescued the expression of Wnt pathway target genes. Furthermore, the expression of RSPO2, a WNT11 target involved in bone cell differentiation, and its receptor leucine-rich repeat containing G protein-coupled receptor 5 (LGR5), was decreased in WNT11 mutant cells. Treatment with WNT5A and WNT11 recombinant proteins reversed LGR5 expression, but Wnt family member 3A (WNT3A) recombinant protein treatment had no effect on LGR5 expression in mutant cells. Moreover, treatment with recombinant RSPO2 but not WNT11 or WNT3A activated the canonical pathway in mutant cells. In conclusion, we have identified WNT11 as a new gene responsible for EOOP, with loss-of-function variant inhibiting bone formation via Wnt canonical and non-canonical pathways. WNT11 may activate Wnt signaling by inducing the RSPO2-LGR5 complex via the non-canonical Wnt pathway.

Introduction

Early onset osteoporosis (EOOP) is defined by low bone mineral density (BMD), which increases the risk of fractures. EOOP is a rare type of osteoporosis that affects children and young adults below age 55 years, without any secondary causes. The prevalence of EOOP is unknown, but the low number of patients reported in cohorts suggests a low prevalence. EOOP and other rare monogenic diseases now appear to be a continuum of the same phenotype. Indeed, the heritability of BMD is high, which indicates a strong genetic background (1–4). Genome-wide association studies revealed >500 significant loci affecting BMD values, whose heritability reached 50–85%; commonly tested genes explained 20% of the variance (5,6).

In EOOP, several genes have been characterized, with a large predominance of genes involved in Wnt pathways (7–12). Wnt signaling is a key regulator of osteoblast differentiation and maturation in both humans and animal models (13,14), mediated by the canonical Wnt/ β -catenin and non-canonical signaling pathways. Both pathways are crucial in regulating osteoblastogenesis and bone formation (15–18). These skeletal functions include several frizzled class receptors (FZDs) and their co-receptors low-density lipoprotein receptor-related protein 5/6 (LRP5/6), but also other transmembrane proteins, R-spondins (RSPOs) or secreted frizzled-related proteins (SFRPs) (19–21).

To date, 19 Wnt ligands have been found related to bone and joints (22). The first described in osteoporosis

Received: September 13, 2021. Revised: November 30, 2021. Accepted: December 2, 2021

© The Author(s) 2021. Published by Oxford University Press. All rights reserved. For Permissions, please email: journals.permissions@oup.com

This is an Open Access article distributed under the terms of the Creative Commons Attribution Non-Commercial License (<http://creativecommons.org/licenses/by-nc/4.0/>), which permits non-commercial re-use, distribution, and reproduction in any medium, provided the original work is properly cited. For commercial re-use, please contact journals.permissions@oup.com

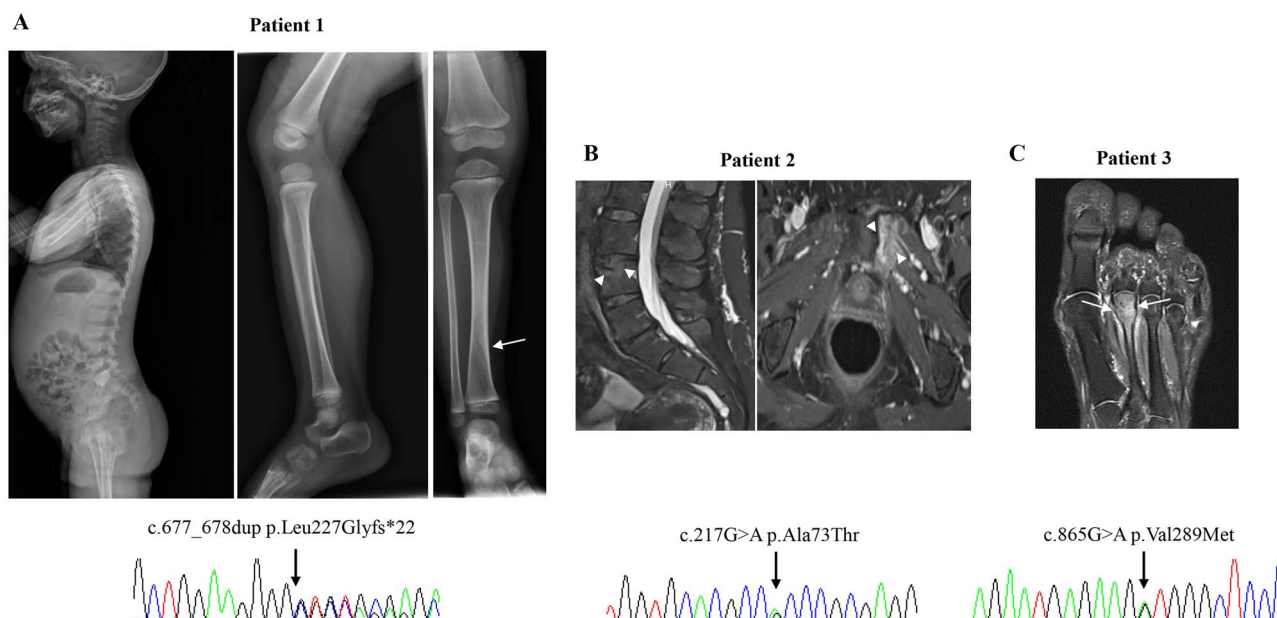


Figure 1. Imaging and electropherogram of the patients. **(A)** Patient 1: 3-year-old boy. X-rays of spine show diffuse osteopenia without vertebral fractures. X-rays of tibia revealed diffuse osteopenia with thin cortical long bones, with a non-displaced spiral fracture of the diaphysis of the right tibia (white arrow) and Sanger sequencing chromatogram. **(B)** Patient 2: 51-year-old woman. Mild fracture of L4 upper vertebral endplate associated with intracancellous herniation on MRI (Oct 2019) and bone-marrow edema as mild hyperintensity on STIR images (white arrowheads) and Sanger sequencing chromatogram. **(C)** Patient 3: 61-year-old woman. Multiple fractures of the metatarsus with bone-marrow edema (white arrows) and Sanger sequencing chromatogram.

was Wnt family member 3A (*WNT3A*), which activates the β -catenin/canonical pathway via *LRP5* binding (12,23). *WNT1* is the most well-known and the main Wnt ligand related to bone fragility and EOOP, which mutations in this gene were described to be related with autosomal dominant osteoporosis (24–26). Other Wnt family members might contribute to low BMD and EOOP, although the molecular pathway is not clearly defined. Wnt family member 11 (*WNT11*), a very conserved gene, is involved in the development of skeleton, kidney, heart and lung (27) and regulates osteoblast maturation *in vitro* (28,29) but was never reported as a disease-causing gene in humans.

By whole-exome sequencing (WES) approach, we found a loss-of-function variant in *WNT11* associated with EOOP in a young boy with osteoporosis and two variant of uncertain significance (VUS) in two non-related women with bone fragility. We then investigated the function of *WNT11* in bone cells by using CRISPR-Cas9 technology to generate cells with a loss-of-function variant. Here, we demonstrate that heterozygous *WNT11* mutation decreased the proliferation of osteoblasts and mineralization nodules and inhibited the expression of target genes of the Wnt canonical and non-canonical pathways. Our results show that *WNT11* significantly contributes to bone homeostasis and that the identified loss-of-function variant is able to cause osteoporosis.

Results

Clinical and molecular characteristics

Patient 1 was a 4-year-old boy [height: 100 cm (Z-score: 0) weight: 15.7 kg (Z-score: 0) bone age corresponded

to chronological age] who experienced several severe fractures after simply falling down. The first fracture occurred at age 3 and was a non-displaced spiral fracture of the diaphysis of the right tibia (Fig. 1A). Six months later, he fractured his left femoral metaphysis. Cognitive function, learning skills and growth were normal. No family history of bone fragility was found. Physical examination was unremarkable, in particular no blue sclera, no teeth abnormalities and no joint laxity. No secondary cause of bone fragility was found, such as endocrine or metabolism deficiencies, and cardiac ultrasonography was normal. No cardiac problems or structural eye abnormalities were observed. X-rays revealed diffuse osteopenia at the vertebra and thin cortical areas of the long bones (Fig. 1A). Dual-energy X-ray absorptiometry (DXA) revealed low BMD at the lumbar spine [0.478 g/cm², Z-score – 2 standard deviation (SD)]. Serum mineral levels were normal. However, for serum bone markers, levels were low for total alkaline phosphatase (117 IU/L; reference values: 129–417 IU/L) and bone alkaline phosphatase (BAP) (45 IU/L; reference values: 66–153 IU/L), but normal for a bone resorption marker [C-terminal telopeptide (CTX) 1158 pg/ml, reference values: 470–1880]. No variants were found assessing the genetic cause of EOOP with our sequencing panel of genes related to bone fragility. Therefore, WES was performed and allowed for identifying a *de novo* heterozygous mutation in *WNT11*, NM_004626.2:c.677_678dup, p.(Leu227Glyfs*22), which was confirmed by Sanger sequencing (Fig. 1A). The average targeted region depth was 112 fold and 99.7% was covered by at least 25 reads, indicative of high quality of WES sequencing. No other variants in genes

Table 1. Molecular characteristics of the WNT11 variants

	Patient 1	Patient 2	Patient 3
Genomic position NG_046931.1	chr11:g.75902820_75902821dup	chr11:g.75907629C > T	chr11:g.75902633C > T
NM_004626.2	c.677_678dupGG	c.217G > A	c.865G > A
protein NP_004617.2	p.(Leu227Glyfs*22)	p.(Ala73Thr)	p.(Val289Met)
Gnomad African	–	0.0040%	0.0000%
Gnomad Asian	–	0.0000%	0.0000%
Gnomad non-Finnish European	–	0.00078%	0.0026%
ClinVar	No	No	No
dbSNP	No	rs 376706959	rs368098788
1000Genomes	No	No	No
CADD Phred	–	24.3	22.5
Polyphen-2	–	Probably damaging	Benign
SIFT	–	Deleterious	tolerated
MutationTaster	–	Disease causing	Disease causing
ACMG classification criteria	PS2, PM2	PM2, PP3	PM2, BP4
ACMG classification	Likely pathogenic	VUS	VUS

related to bone fragility were found in the WES, including ALPL. The WNT11 mutation was not found in gnomAD, 1000Genomes or dbSNP databases. The probability of loss-of-function intolerance of this gene from GnomAD is 0.01, and the loss-of-function observed/expected upper bound fraction as LOEUF is 0.81. The molecular characteristics of the variant are summarized in Table 1.

Patient 2 was a 51-year-old woman with bone fragility. She had a wrist fracture at age 42, pelvis and two vertebral lumbar fractures (Fig. 1B) at age 49 and several toe fractures, all under low trauma conditions. She reported a history of surgery for lumbar spinal stenosis. She had no dental or audition problems. DXA revealed osteoporosis (lumbar spine T-score – 3.3 SD, Z-score – 2.6 SD; femoral neck T-score: –3.8 SD, Z-score –3.1 SD). magnetic resonance imaging (MRI) revealed lumbar osteoarthritis in addition to the vertebral fracture. Biological tests gave normal results, including serum levels of calcium, phosphorus, alkaline phosphatase, BAP, CTX, procollagen type I N-terminal propeptide (PINP), osteocalcin, tartrate-resistant acid phosphatase 5b (TRAP5b), sclerostin and 25-OH vitamin D (25OH) vitamin D. Patient 2 was not fully menopausal, but with irregular menses. She was not taking any hormone replacement therapy, in particular no estrogens. The bone fragility NGS panel, which included WNT11 since the discovery of the variant in the boy, was used to search for genetic variants. The woman carried a missense variant in WNT11 NM_004626.2: c.217G > A p.(Ala73Thr), rs376706959 (Fig. 1B). Her 69-year-old mother had several osteoporotic fractures; she carried the same heterozygous variant, which therefore probably segregates with the phenotype. According to the gnomAD database, the allele frequency of this variant is very low in African (0.0040%) and non-Finnish European (0.00078%) populations and in all populations (0.0014%). The prediction software combined annotation-dependent depletion (CADD) presented a PHRED at 24.3, Polyphen2, sorting intolerant from tolerant (SIFT) and Mutation Taster consider this variant as probably damaging, deleterious and disease-causing, respectively, with high probability

scores. Also, according to the American College of Medical Genetics (ACMG) classification, this variant was considered as a VUS (Table 1).

Patient 3 was a 61-year-old woman with no risk factors for osteoporosis and no family history of fracture. She had no dental problems but had worn ear devices from age 59. The etiology of the hearing impairment is unknown and further investigation is needed in a context of a family history of hearing loss. She reported lumbar spine osteoarthritis. When she was 55 years old, she had fractures of the 3rd and 4th left metatarsi and 2 months later the 2nd left metatarsus, without trauma. A few months later, she had fractures of the 2nd, 3rd and 4th right metatarsi (Fig. 1C). On DXA, the lumbar spine BMD T-score was –1.4 SD and Z-score 0.32 SD and femoral neck T-score –0.3 SD and Z-score 1.18 SD. Levels of all serum biomarkers were within the normal range for a postmenopausal woman. She carried a missense variant in WNT11 (NM_004626.2: c.865G > A p.(Val289Met) rs368098788) (Fig. 1C). According to the gnomAD database, the allele frequency of this variant is very low (all populations: 0.0012%; non-Finnish Europeans: 0.0026%). The polyphen2 and SIFT prediction software consider this variant as benign and tolerated, respectively; the CADD with a PHRED at 22.5 was classified as probably pathogenic as was the Mutation Taster score. Also, according to the ACMG algorithm, this variant was classified as a VUS (Table 1).

WNT11 loss-of-function variant decreased cell differentiation, mineralization and proliferation

To investigate the functional properties and to confirm that the pathogenicity of the identified variant could result in the osteoporotic phenotype, we generated a mutation in U2OS cells by using the CRISPR-Cas9 technique. We designed a guide RNA (gRNA) followed by a protospacer adjacent motif sequence that targeted the same region as the loss-of-function variant in WNT11 (NM_004626.2:c.677_678dup p.Leu227Glyfs*22) carried by patient 1. A heterozygous variant with a 32-base pair deletion (NM_004626.2:c.690_721dels*40) was generated

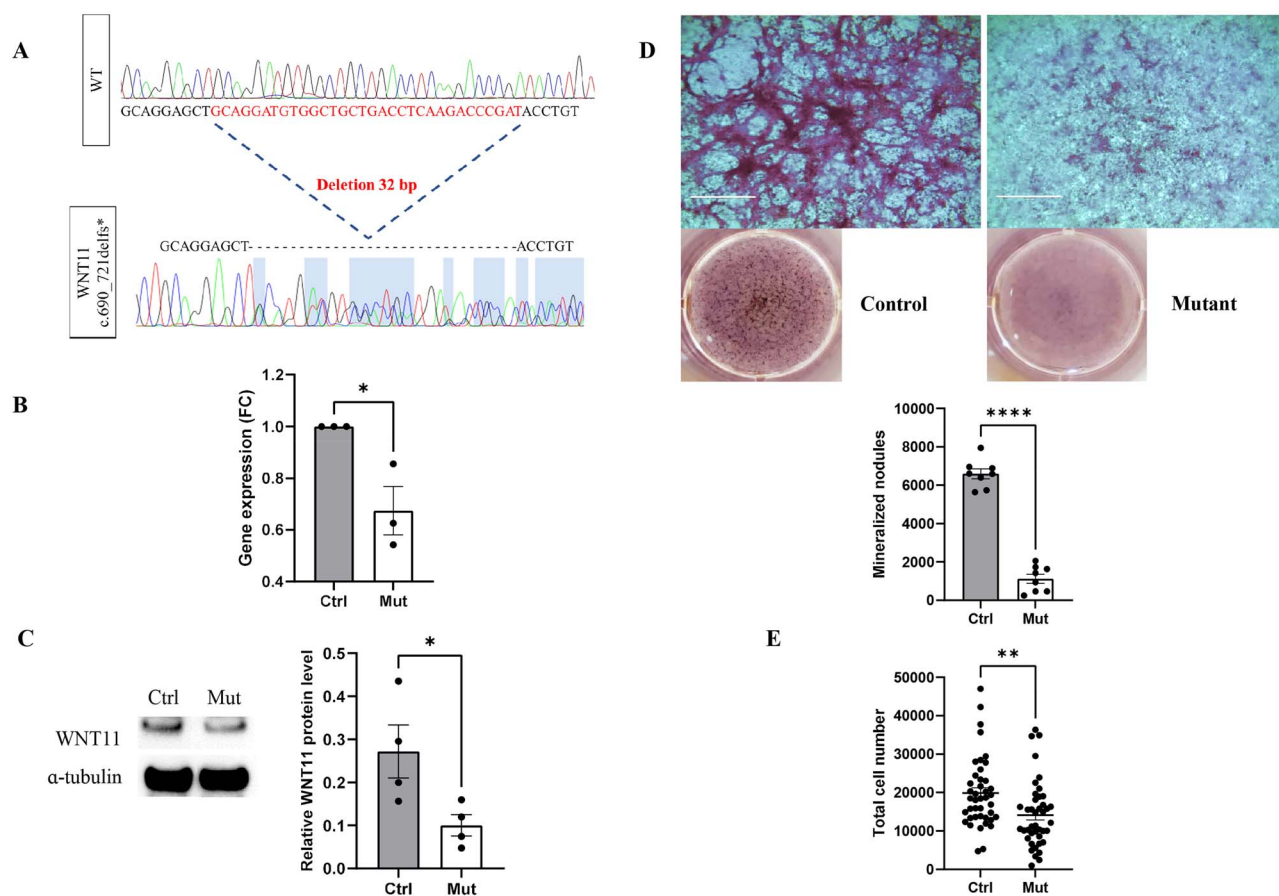


Figure 2. WNT11 heterozygous mutant cells with decreased WNT11 mRNA and protein levels as well as proliferation and mineralization. (A) Electropherogram showing the 32-bp deletion leading to a frameshift. fs*: frameshift. (B) RT-qPCR analysis of WNT11 mRNA expression in mutant versus control U2OS cells. Normalization was to GAPDH level as a housekeeping gene with ratio of one for control U2OS cells. Ctrl: wild-type U2OS cells, Mut: WNT11 mutant cells, FC: fold change. (C) Western blot analysis of WNT11 protein expression, confirming the heterozygosity. α -Tubulin was a control. (D) Alizarin red staining showed formation of mineralized nodules after osteogenic differentiation treatment with osteogenic media in control and WNT11 mutant cells. (E) Proliferation of control and WNT11 mutant cells ($n = 42$). Data are mean \pm SEM. * $P < 0.05$, ** $P < 0.01$, **** $P < 0.0001$.

in U2OS cells (Fig. 2A), which resulted in decreased WNT11 mRNA and protein levels (Fig. 2B and C). We then investigated osteoblast differentiation and mineralization as well as proliferation in WNT11 mutant and control cells. With osteogenic differentiation treatment, WNT11 mutant cells formed 80% less mineralized nodules than control cells ($P < 0.0001$, Fig. 2D). Proliferation assay revealed 30% decreased proliferation in WNT11 mutant cells as compared with control cells ($P < 0.05$, Fig. 2E). WNT11 mutant cells when treated with rhWnt11, display a rescue in the proliferation but not in the mineralization (Supplementary Material, Fig. S1). No significant difference was seen when control cells were treated with rhWnt11.

Together, these results suggest that WNT11 controls proliferation, differentiation and mineralization in osteoblasts.

Loss-of-function variant in WNT11 reduced the gene expression of osteoblast differentiation markers and genes of the WNT canonical and non-canonical pathways

To gain insight into the mechanism of impaired bone formation in WNT11 mutant cells, we examined the mRNA

levels of osteoblast differentiation genes: RUNX2, as a common target of Wnt pathways; Osterix (SP7); integrin-binding sialoprotein (IBSP); osteocalcin (BGLAP) and collagen type I (COL1A1). As compared with control wild-type U2OS cells, WNT11 mutant cells showed reduced mRNA levels of RUNX2 and the RUNX2 target genes SP7, IBSP and BGLAP, which regulate bone mineralization (Fig. 3A). The expression of COL1A1 and ALPL was not affected.

To better understand the effect of WNT11 in bone cells, we investigated the mRNA levels of major genes related to the Wnt pathways. WNT11 mutant cells showed decreased expression of genes in both the canonical (β -CATENIN, LRP5) and non-canonical (JUN, MAPK9, ROR2) Wnt pathways (Fig. 3B) relative to control cells. RUNX2, ROCK1, OPG and RANKL, indirect targets for the two Wnt pathways, were also downregulated. To verify the specificity and causality of the WNT11 mutation, we tested rescue of the mutation effects by adding rhWnt11 in cultures of WNT11 mutant cells (Fig. 3B) and control cells (Supplementary Material, Fig. S2). RhWnt11 restored the mRNA expression of RANKL and OPG as well as the non-canonical pathway genes RUNX2, MAPK9 and ROR2. Neither JUN nor ROCK1 indirect target gene expression was rescued, nor was that of the

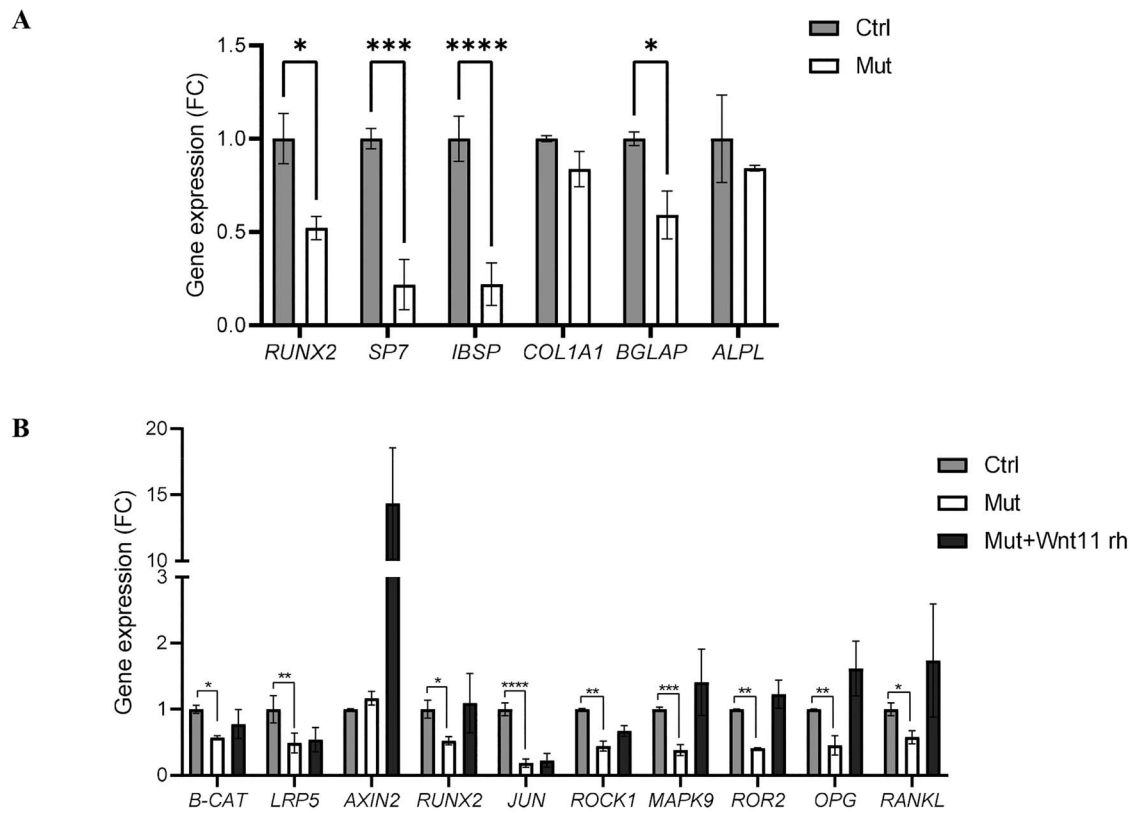


Figure 3. Expression of osteoblast differentiation markers and genes from the canonical and non-canonical Wnt pathways is decreased in WNT11 mutant cells. RT-qPCR analysis of mRNA levels of (A) osteoblast differentiation genes and (B) genes of the Wnt canonical and non-canonical pathways in control cells and in WNT11 mutant cells with and without Wnt11 recombinant protein treatment. Ctrl: control, Mut: WNT11 mutant cells, Mut+rhWnt11: WNT11 mutant cells treated with rhWnt11. Data are mean \pm SEM. * $P < 0.05$, ** $P < 0.01$, *** $P < 0.001$, **** $P < 0.0001$.

canonical pathway genes *LRP5* and β -CATENIN. However, the expression of *AXIN2*, coding for an inhibitor of the canonical Wnt pathway, was unaffected by the WNT11 mutation but was greatly induced by rhWnt11 in mutant cells. These results suggest that the impaired differentiation was mediated by the heterozygous WNT11 mutation affecting both canonical and non-canonical Wnt pathways.

WNT3A did not activate the canonical pathway in WNT11 mutant cells

To confirm that the canonical Wnt/ β -catenin pathway is impaired in the WNT11 mutant versus control cells, we analyzed the translocation of β -catenin into the nucleus by immunofluorescence assay. Under basal conditions, β -catenin was localized in the membrane and cytoplasm in both cell lines (Fig. 4A and F). We then treated both cell lines with rhWnt3a, rhWnt5a and rhWnt11. RhWnt3a activated the canonical pathway in control cells, as illustrated by β -catenin nuclear translocation, but not in WNT11 mutant cells (Fig. 4B and G), not activating the canonical pathway. In addition, we observed no β -catenin translocation in control or WNT11 mutant cells treated with rhWnt5a (Fig. 4C and H) or rhWnt11 (Fig. 4D and I). Treatment with rhWnt11 alone was not sufficient to activate β -catenin. However, mutant cells simultaneously treated with rhWnt11 and rhWnt3a showed a recovery

that resulted in increased β -catenin expression and its transactivation into the nucleus, which indicates activation of the canonical Wnt pathway (Fig. 4E and J).

To confirm the absence of canonical activity induced by rhWnt3a or rhWnt11 alone and the activation of the canonical activity when treated in combination rhWnt3a+rhWnt11 in mutant cells, we tested a t cell factor/lymphoid enhancer factor (TCF-LEF) reporter plasmid in luciferase activity assay under stimulation with rhWnt3a or rhWnt11 and rhWnt3a+rhWnt11 simultaneously (Fig. 4K). RhWnt3a reduced the activation by 90% in mutant cells as compared with rhWnt3a activating the Wnt canonical pathway in control cells, rhWnt11 conferred no activation in control or mutant cells and rhWnt3a+rhWnt11 together do not present a significant difference between control and mutant, differently from the Wnt3a treatment alone. These results suggest that WNT11 alone does not directly control the canonical pathway but may facilitate its activation induced by WNT3A.

WNT11 mutation decreases RSPO2 and LGR5 expression

To further investigate the function of the WNT11 mutation, we wondered whether its effect could be driven by R-Spondin 2 (RSPO2), an activator of the canonical Wnt signaling pathway. In osteoblasts, RSPO2

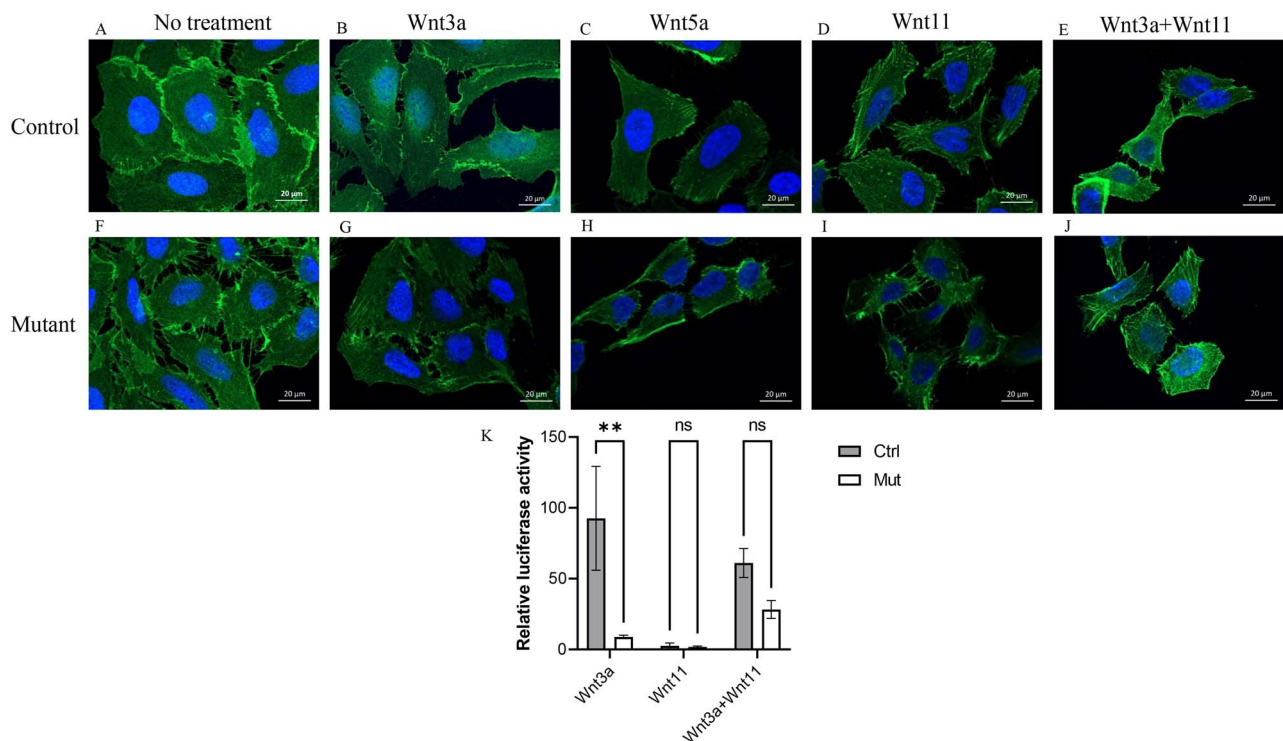


Figure 4. WNT11 mutation severely impedes β -catenin translocation and activation of the canonical Wnt pathway. (A–J) Immunofluorescence detection of β -catenin (green), in wild-type control (A–E) and WNT11 mutant (F–J) U2OS cells; blue is DAPI counterstaining for cell nucleus. The cells were untreated (A, F) or treated with rhWnt3a (B, G), rhWnt5a (C, H), rhWnt11 (D, I) or rhWnt3a and rhWnt11 (E, J). (K) Control and mutant cells were transfected with the TCF-LEF TOPflash vector and treated with rhWnt3a, rhWnt11 or rhWnt3a + rhWnt11 simultaneously. Data represent normalized luciferase activity relative to untreated cells. Data are mean \pm SEM. ** $P < 0.01$.

acts as a ligand for LGR4–6 receptors and is known to promote osteoblast maturation and mineralization via WNT11 (26). The expression of RSPO2 was decreased by 55.8% in WNT11 mutant cells as compared with control cells ($P < 0.01$) (Fig. 5A). To determine the relation between WNT11 and RSPO2, we next investigated the expression of the RSPO2 receptors in WNT11 mutant cells. The expression of LGR5 but not LGR4, LGR6 or ZNRF3 receptors was significantly lower in WNT11 mutant than control cells ($P < 0.05$, Supplementary Material, Fig. S3). To investigate whether the Wnt canonical or non-canonical pathway induced LGR5 expression in mutant cells, we treated cells with rhWnt3a, rhWnt5a and rhWnt11 (Fig. 5B). The expression of LGR5 was downregulated in WNT11 mutant cells and was reversed by exogenous rhWnt11 and rhWnt5a but not rhWnt3a treatment (Fig. 5B). To further investigate the functional role of RSPO2 in WNT11 mutant cells, we exposed cells to exogenous rhRspo2 before immunofluorescence and luciferase activity experiments. On immunofluorescence assay, the addition of rhRspo2 promoted the nuclear translocation of β -catenin only in control cells (Fig. 5C). However, rhRspo2 induced activation of the canonical pathway in both WNT11 mutant and control cells as illustrated by luciferase assay (Fig. 5D). This was not observed with rhWnt3a, which failed to activate the canonical pathway in WNT11 mutant cells (Fig. 4K), which suggests that WNT11 controlled the canonical pathway via RSPO2. Our data show that the WNT11

loss-of-function variant may cause EOOP by regulating Wnt pathways, in particular by decreasing signaling via RSPO2 binding to LRG5 receptors (Fig. 5E).

Discussion

Here, we identified for the first time a WNT11 loss-of-function variant associated with EOOP, which contrasts with the previous idea that WNT11 could be a candidate gene for high bone mass (30). Indeed, two of the three patients presenting a heterozygous, potentially inactivating mutation in WNT11 displayed low bone mass with vertebral and/or long bone fractures, whereas patient 3 presented many unusual fractures despite the absence of low BMD. According to the ACMG guidelines, the results of the functional analysis performed in bone cell model and the presence of an undescribed *de novo* frameshift variant suggest that the variant carrying by patient 1 is likely pathogenic in osteoporosis (31). Moreover, the three patients with WNT11 mutations did not show any alterations in other organs, in contrast to what was reported in animal models with mutations in the same gene (32–35).

WNT11 has been found involved in early development in mice, the *Xenopus* frog and zebrafish (32–35). For example, homozygous zebrafish carrying a point mutation in *wnt11* (silberblick slb tx226) exhibit altered eye formation and partial fusion of the eyes (36). In the *Xenopus* frog, Wnt11 is required for heart

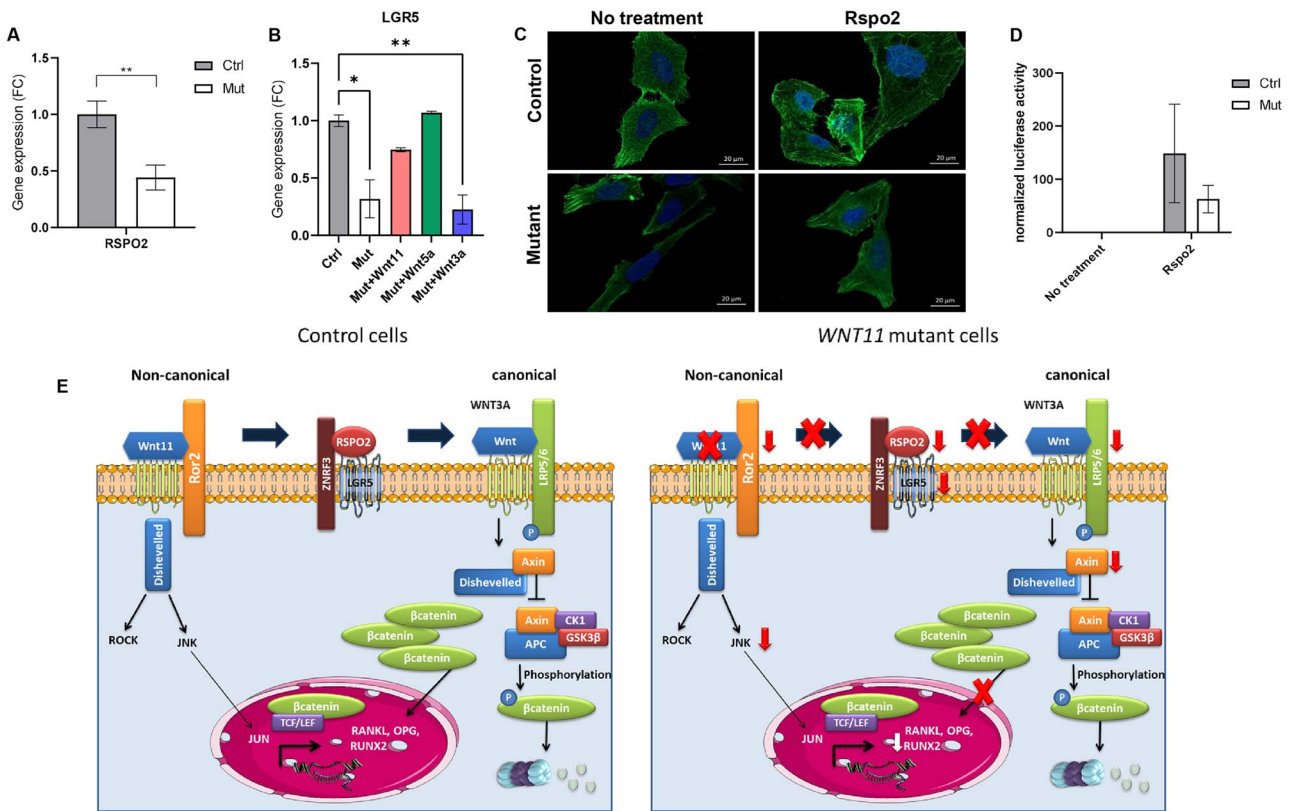


Figure 5. Wnt non-canonical pathway controls RSPO complex, which controls Wnt canonical pathway. RT-qPCR analysis of mRNA level of (A) RSPO2 and (B) LGR5 with rhWnt3a, rhWnt5a and rhWnt11 treatment. Data are mean \pm SEM. * $P < 0.05$, ** $P < 0.01$. (C) Immunofluorescence assay of cells treated with rhRspo2; blue (DAPI) and green (β -catenin). (D) Luciferase activity of control and WNT11 mutant cells with rhRspo2 treatment. Ctrl: control, Mut: WNT11 mutant cells. (E) Scheme summarizing the effect of WNT11 in normal cells (left) and heterozygous WNT11 mutation with red symbols (right): WNT11 is a ligand of the Wnt non-canonical pathway; thus, WNT11 mutation decreased the expression of genes in the non-canonical Wnt pathway as well as RSPO2 and LGR5. LGR5 expression is rescued upon Wnt non-canonical but not canonical ligand treatment. Lack of WNT11 decreased the expression and activation of genes in the canonical Wnt pathway, which was reversed by treatment with rhRspo2.

morphogenesis (34), and Wnt11 inactivation induced myocyte proliferation in perinatal mouse hearts (32). To this date, Wnt11 knock out mouse was only studied at homozygous level, which leads to a severe cardiac phenotype (32) and this model has not been explored at heterozygous level and neither the bone phenotype. Our patients with WNT11 variants showed only osteoporosis, with no additional comorbidities, which possibly reflects haploinsufficiency in the heterozygous individuals. In addition, the phenotype of patients with pathogenic WNT11 variants diverged from that of patients with osteoporosis caused by loss-of-function variants in LRP5 (23) or the proto-oncogene WNT1 (37), showing mostly vertebral fractures and low BMD at the spine.

Functional studies in our heterozygous mutant cell line showed that WNT11 is required for proliferation, osteogenic differentiation and mineralization. WNT11 has been reported to promote osteogenic differentiation in different cell models, such as bone-marrow mesenchymal stem cells and murine sarcoma cells (C3H10T1/2 cells) (28,38). To confirm that the identified WNT11 loss-of-function variant would cause the observed osteoporotic phenotype and to study their impact on the Wnt canonical and non-canonical pathways, we used a CRISPR-Cas9 approach to generate heterozygous WNT11

mutant U2OS cells. The heterozygous frameshift mutation generated in the cells, very close to the mutation in patient 1, allowed us to confirm that the loss-of-function WNT11 variant is associated with a bone fragility phenotype. Our results revealed decreased cell proliferation in WNT11 mutant cells similar to previous studies showing that WNT11 stimulated proliferation in breast cancer cells and small cell lung cancer (39,40). Moreover, the mutant cell line showed decreased osteogenic differentiation and mineralization, as illustrated by alizarin red staining of differentiating cells (Fig. 2D) and decreased expression of osteoblast marker genes (Fig. 3A). Indeed, the level of RUNX2, a target of both Wnt pathways, was decreased, as was the expression of BGLAP ($P < 0.05$), SP7 ($P < 0.001$) and IBSP ($P < 0.0001$), which suggests that WNT11 promotes osteoblast differentiation. In addition, the lack of change in expression in COL1A1 and ALPL in WNT11 mutant cells suggests that WNT11 does not regulate bone formation alone. Here, we did not find a significant decrease in ALPL mRNA level, which might be related to U2OS cells exhibiting lower levels of basal and primed alkaline phosphatase activity than other cell models (41). However, serum level of BAP was low in patient 1, which suggests decreased bone formation and agrees with our *in vitro* findings.

We found that the pathogenic heterozygous deletion in *WNT11* inhibited both the non-canonical and canonical Wnt pathways. The expression of specific genes involved in the canonical (*LRP5*, *B-CAT*) and non-canonical (*JUN*, *MAPK9*, *ROR2*) pathways was downregulated; exposure to exogenous rhWnt11 rescued only the non-canonical marker genes *MAPK9* and *ROR2*.

Similarly, *WNT11* mutant cells treated with rhWnt11 did not show a rescue for mineralization (Supplementary Material, Fig. S1), which is a complex biological process and requires the canonical pathway (42). Also, there is no full activation of the canonical Wnt pathway in *WNT11* mutant cells treated with rhWnt3a; hence, *WNT11* might be upstream of *WNT3A* signaling and may positively control the canonical pathway. Exposure to rhWnt11 alone did not activate β -catenin nuclear translocation in mutant cells or the canonical pathway reporter genes (Fig. 4). However, β -catenin expression and translocation into the nucleus and canonical activity were increased with rhWnt11 and rhWnt3a treatment combined (Fig. 4E, J and K) in mutated cells which further support that *WNT11* is required for activation of the canonical pathway. We also observed that there was no significant difference between mutant and control cells on the canonical activity after the rhWnt11 and rhWnt3a simultaneous treatment. This observation was associated with a lower canonical activity for control cells as compared with rhWnt3a treatment alone. This result may happen because simultaneous treatment led to a complex effect not allowing a full activation of canonical pathway. This tricky effect could reflect *WNT11* as an inhibitor function on the canonical pathway that has been already described in other models (43,44).

Such a crosstalk between Wnt ligands was shown during mouse embryonic development, with the *Wnt5a* ligand, which mainly drives the non-canonical pathway, possibly having positive or negative regulatory effects on *WNT*/ β -catenin signaling. This effect depends on the cell type and their specific expression of the receptors (43,45). Partial inhibition of the canonical Wnt signaling cascades by *WNT5A* was also reported in cancer cells (45,46) and cardiomyocytes (47). Here, we show that *WNT11* promotes bone formation via *ROR2*/*JNK* signaling and inhibits the Wnt canonical pathway.

Indeed, rhWnt11 strongly increased the expression of *AXIN2* in *WNT11* mutant but not wild-type cells (Supplementary Material, Fig. S2). *AXIN2* protein is a repressor of the canonical pathway (48). This increase in *AXIN2* expression may explain why treatment with rhWnt11 did not rescue the expression of canonical pathway genes (*B-CATENIN* and *LRP5*). The striking induction of *AXIN2* in the presence of rhWnt11 strongly suggests that *WNT11* has a role in the canonical pathway.

Here, we observed a decrease in mRNA levels of *OPG* and *RANKL* in *WNT11* mutant cells and a recovery of both levels in the presence of rhWnt11. Both genes likely have

an effect on osteoclastogenesis, as was described for the *WNT16A* ligand (49).

Respondins (RSPOs) are a family of regulators of Wnt pathways (50). *RSPO2* activates the canonical Wnt pathway by acting as a ligand for *LGR4–6* receptors and also regulates both the canonical Wnt/ β -catenin-dependent and non-canonical Wnt pathways by inhibiting *ZNRF3* (51–53). *RSPO2* promoted osteoblast maturation and mineralization in knockout mice (54) and mediated Wnt11-dependant osteoblast differentiation in murine MC3T3 cells (29). In agreement with these observations, we also observed reduced *RSPO2* expression in *WNT11* mutant cells. In addition, *LGR5* expression was decreased in our model, but *LGR4*, *LGR6* and *ZNRF3* levels remained unchanged (Supplementary Material, Fig. S3). Previous findings show that *WNT5A* directly stimulates the expression and production of *LGR5* (55) in human osteoarthritic osteoblasts. Accordingly, we observed that rhWnt5a and rhWnt11 but not the canonical Wnt pathway activator rhWnt3a restored *LGR5* expression in *WNT11* mutant cells. Finally, exogenous rhRspo2 activated the Wnt canonical pathway in both wild-type and *WNT11* mutant cells (Fig. 5D), but rhWnt3a did not in the absence of rhWnt11. These results suggest that *WNT11*, possibly cooperating with *WNT5A*, activates Wnt signaling by inducing the *RSPO2–LGR5* complex via the non-canonical Wnt pathway (Fig. 5E).

In conclusion, we describe the association of *WNT11* heterozygous loss-of-function variant and *EOOP*, with *WNT11* acting by inhibiting the canonical and non-canonical Wnt pathways, thus decreasing cell proliferation and osteoblastic differentiation. We provide evidence that *WNT11* acts, at least in part, by triggering *RSPO2* signaling, thus activating the canonical pathway (Fig. 5E). *WNT11* might be a candidate target gene for the development of bone anabolic drugs in osteoporosis.

Materials and Methods

Patients

Three patients were referred to an academic reference center of bone diseases because of unusual presentation of bone fragility. The three individuals had fractures without any other additional clinical signs that could indicate secondary causes of osteoporosis. They had no history of chronic inflammatory diseases or eating disorders. Secondary causes of osteoporosis were also ruled out by biological tests, including blood cell count; measuring serum levels of C-reactive protein, total creatinine, calcium, phosphorus, 25OH vitamin D, thyroid-stimulating hormone, parathyroid hormone, and prolactin; and electrophoresis of proteins. After negative results for secondary causes, a molecular analysis was performed to investigate the hypothesis of a monogenic bone disorder. This approach was approved by the French Ethics Committee and patients gave their written informed consent for genetic tests.

Bone biomarkers

Serum carboxy-terminal collagen crosslink (CTX), 25OH vitamin D, osteocalcin and P1NP levels were measured by using automated electrochemiluminescence immunoassay systems (Cobas 8000 modular analyzer series, Roche Diagnostics, Meylan, France). Serum total alkaline phosphatase was measured with an Alinity instrument (Abbott diagnostics, Rungis, France). The Quidel enzyme immunoassay (San Diego, CA) was used to determine BAP level. Enzyme-linked immunoassay was used to determine serum levels of TRAP5b (Immunodiagnostic Systems, Pouilly-en-Auxois, France) and sclerostin (TECOmedical, Sissach, Switzerland).

DXA

BMD at the lumbar spine was measured by DXA using a Lunar Prodigy device (GE Healthcare, Piscataway, NJ). The BMD results were transformed to age- and sex-specific Z-score using data published by Manousaki *et al.* (56) for patients under 4.5 years old.

WES

Exome capture involved using the Integragen platform (Évry, France) with the Human Core Exome kit (Twist Bioscience, San Francisco, CA). Paired-end sequencing was performed on a NovaSeq analyzer (Illumina, San Diego, CA) generating 2×150 pb. Sequence data were analyzed and visualized via the Sirius interface (Integragen, Évry, France). For sequence alignment, variant calling and annotation, sequences were aligned to the human genome reference sequence (UCSC Genome Browser, hg38 build) by using the burrows-wheeler alignment aligner. Downstream processing involved the Genome Analysis Tool kit, SAMtools and Picard Tools.

Targeted gene sequencing and Sanger sequencing

After WES, which identified WNT11, we included this gene in the targeted gene-sequencing panel for bone fragility: BMP1 (NG_029659.1), COL1A1 (NG_007400.1), COL1A2 (NG_007405.1), CRTAP (NG_008122.1), CREB3L1 (NG_033264.1), DKK1 (NC_000010.11), FKBP10 (NG_015860.1), IFITM5 (NG_032892.1), LRP5 (NG_015835.2), LRP6 (NG_016168.2), PLS3 (NG_012518.2), P3H1 (NG_008123.1), SERPINF1 (NG_028180.1), SP7 (NG_023391.2), WNT1 (NG_033141.1), WNT3A (NC_000001.11), WNT11 (NG_046931.1) and WNT16 (NG_029242.1). NGS involved using the surelectQXT kit (Agilent, Les Ulis, France) for library preparation and the hybrid capture system for sequencing on a Miseq sequencer (Illumina, San Diego, CA). Sequence results were obtained after aligning fastqs, mapping and variant calling by using SeqNext software (JSI Medical Systems, Ettenheim, Germany). SeqNext is based on Smith–Waterman (57) and Burrows Wheeler Aligner algorithms (58). The copy number variations were also determined by using this software. For each exon, the coverage was 100% at 30×. The highest minor

allele frequency of variants was investigated with the databases 1000 Genomes phase 3 (<ftp://ftp.1000genomes.ebi.ac.uk/vol1/ftp/phase3/data>) and gnomAD (<https://gnomad.broadinstitute.org/>); the filtering criteria were maximum MAF < 0.05% corresponding to the definition of rare disease in the European Union.

Sanger sequencing confirmed the potentially pathogenic variants identified in the panel by using Life Technologies reagents and software on an ABI3130 sequencer (Thermo Fisher, Les Ulis, France). Variant pathogenicity was evaluated by using Alamut (SOPHiA Genetics, Lausanne, Switzerland) including variable in silico predictive software (SIFT, MutationTaster and PolyPhen 2) and CADD (<https://cadd.gs.washington.edu>).

Generation of mutant cells by CRISPR-Cas9

Human osteosarcoma cells (U2OS) were purchased from ATCC (Manassas, VA). The WNT11 CRISPR-Cas9 knockout cell line was generated by using TrueGuide Synthetic CRISPR gRNA Thermo Fisher (Waltham, MA), with the target sgRNA sequence CAAGACCC-GATACCTGTCCG. Heterozygous knockout was confirmed by Sanger sequencing of the genomic DNA. The genomic DNA was isolated from wild-type U2OS and WNT11 knockout cells. The gRNA targeted area was amplified with 5'-AGTGTAAAGTGCCATGGGGTG-3' and 5'-GAATGAGAAGGTGGGCTCCC-3' primers and Sanger sequenced following the manufacturer's protocol (Applied Biosystems, Foster City, CA).

Cell culture and treatment with recombinant proteins

U2OS cells were cultured with McCoy's medium (Sigma, St. Louis, MO) with 10% fetal bovine serum (FBS) and 1% penicillin/streptomycin, in a humidified atmosphere (37°C and 5% CO₂). Experiments were conducted in the presence of Wnt ligands to assess the gene expression and immunofluorescence and luciferase activity. Recombinant proteins were added to the medium of 70% to 90% confluence cells, then cultured for 24 h and harvested for ribonucleic acid (RNA) extraction. Mutant cell lines were treated with recombinant human WNT11 protein (rhWnt11), Chinese hamster ovary derived (CHO derived) (R&D Systems, Minneapolis, MN) for 24 h. Additional experiments were performed in mutant cells cultured with 100 ng/ml recombinant human WNT5A protein (rhWnt5a), CHO derived, and with recombinant human WNT3A protein (rhWnt3a), CHO derived (R&D Systems, Minneapolis, MN) for 24 h. Furthermore, control U2OS cells and mutant WNT11 cells were treated with recombinant human Rspo2 protein (rhRspo2) (from mouse myeloma cell line), rhWnt3a, rhWnt5a and rhWnt11 (100 ng/ml) for 5 h for immunofluorescence analysis. Also, control and WNT11 mutant cells were treated with rhRspo2, rhWnt3a and rhWnt11 for 2 h before transfection for luciferase activity assay.

Proliferation assay

The proliferation assay involved using control and WNT11 mutant cells seeded at 1×10^4 density in a 96-well plate and cultured with DMEM and 10% FBS. Cell numbers were determined 24 h later by CyQuant cell proliferation assay following the manufacturer's protocol (Life Technologies, Carlsbad, CA).

Gene expression analysis

Total RNA was extracted from wild-type U2OS cells, WNT11 mutant cells, and WNT11 mutant cells treated with rhWnt11, rhWnt3a and rhWnt5a (all 100 ng/ml). RNA was extracted by using the RNeasy Mini kit (QIAGEN, Valencia, CA) according to the manufacturer's protocols. The absorbance of RNA was determined at a wavelength of 260 and 280 nm with a NanoDrop-2000 system (Thermo Fisher, Waltham, MA). Complementary DNA (cDNA) was synthesized from RNA by using high-capacity cDNA reverse transcription kit (Applied Biosystems, Foster City, CA) and was used immediately or stored at -20°C . The primers used for reverse transcription polymerase chain reaction are in [Supplementary Material, Table S1](#) and were designed by using the Roche Universal Probe Library Assay Design Center (Basel, Switzerland). The PCR amplification system included the following: $2 \times$ SYBR Green PCR master mix (Applied Biosystems, Foster City, CA), $0.4 \mu\text{M}$ forward and reverse primers, 100 ng cDNA and sterile water for a total volume of $25 \mu\text{l}$. The thermocycling conditions were 95°C for 10 min, 95°C denaturation for 15 s, 60°C anneal/extend for 1 min, for 40 cycles. Dissociation curve analysis was performed at the end of the PCR cycles. Gene expression levels were normalized to GAPDH level in each sample and were determined by the $2^{-\Delta\Delta\text{C}_q}$ method (59). All experiments were repeated three times in duplicate. For some genes, we used a TaqMan probe for specificity reasons.

Total RNA extraction and cDNA synthesis were performed as previously described. TaqMan probes for HPRT, RSPO2 and RSPO4 were from Thermo Fisher (Waltham, MA). The PCR amplification system included the $20 \times$ TaqMan gene expression assay, $2 \times$ TaqMan gene expression master mix (Applied Biosystems, Foster City, CA), 50 ng cDNA template and sterile water for a total volume of $20 \mu\text{l}$. The thermocycling conditions were 50°C for 2 min, 95°C for 10 min, 95°C denaturation for 15 s, 60°C anneal/extend for 1 min, for 40 cycles. Dissociation curve analysis was performed at the end of the PCR cycles. Gene expression levels were normalized to HPRT level in each sample and were determined by the $2^{-\Delta\Delta\text{C}_q}$ method (59). The experiment was performed three times in duplicate.

Osteoblast differentiation and mineralization assay

Cells were seeded at 5×10^4 cells/cm² in 24-well culture plates with Dulbecco's modified eagle medium (DMEM) supplemented with 10% FBS. After 24 h, the culture medium was changed to osteogenic media [DMEM supplemented with 10% FBS, $0.1 \mu\text{M}$ dexamethasone, 10 mM

β -glycerophosphate and $50 \mu\text{M}$ ascorbic acid (all from Sigma, St. Louis, MO)] to induce U2OS cell differentiation. The culture medium was changed twice a week for 18 days. Cells were fixed with 4% paraformaldehyde for 30 min, washed with distilled water and stained with 2% alizarin red for 45 min as described (60).

Western blot analysis

Cells were washed with ice-cold PBS, then lysed with CE buffer [HEPES (10 mM) pH 7.9, KCl (10 mM), EDTA (0.1 mM), NP-40 0.3%, protease inhibitors $1 \times$] and NE buffer [HEPES (20 mM) pH 7.9, NaCl (0.4 M), EDTA (1 mM), glycerol 25%, protease inhibitors $1 \times$] before boiling and loading an equal amount of proteins ($30 \mu\text{g}$) on 12% sodium dodecyl sulphate-polyacrylamide gel electrophoresis gels. The iBlot 2 Gel Transfer Device (Thermo Fisher, Waltham, MA) was used for transfer. After 1-h blocking (5% BSA), the following antibodies were used for detecting proteins: rabbit anti-WNT11 (1:1000, PA5-21712, Thermo Fisher Waltham, MA), goat anti-rabbit IgG H&L horseradish peroxidase (HRP) (ab205718, Abcam, Cambridge, UK) secondary antibody; mouse anti-tubulin (1:10 000, ab7291, Abcam, Cambridge, UK) and m-IgG κ (BP-HRP) (1:2000, sc-516 102, Santa Cruz Biotechnology, Santa Cruz, CA) anti-mouse secondary antibody. Amersham enhanced chemiluminescence (rpn2232) (GE healthcare, Chicago, IL) was used for chemiluminescence detection of protein bands. The experiment was repeated three times and band intensity was quantified by using ImageJ.

Immunofluorescence assay

Cells grown on coverslips were fixed with 4% paraformaldehyde at room temperature for 15 min, then permeabilized with 0.1% Triton for 5 min at room temperature and blocked with 3% BSA for 1 h, washed with PBS and incubated with the anti- β -catenin primary antibody (1:333, ab16051, Abcam, Cambridge, UK) overnight. Cells were washed with PBS, blocked with 3% BSA for 30 min and incubated with secondary antibody for 1 h (1:100, Alexa Fluor 488 goat anti-rabbit antibody, Invitrogen). Cells were washed again with PBS, stained with DAPI for 1 min and mounted on slides. Fluorescence microscopy involved using the microscope ZEISS observer Z1 and ZEN software for analysis (ZEISS, Oberkochen, Germany).

Evaluation of the canonical Wnt pathway activity

Control U2OS and WNT11 mutant cells were seeded in 24-well plates and cultured until 70% to 80% confluence. To investigate whether rhWnt3A, rhWnt11 and rhRspo2 could activate the Wnt canonical pathway in control and WNT11 mutant cells, recombinant proteins were added at 100 ng/ml at 2 h before the transfection. Plasmids for TCF-LEF (67.7 ng), TOPflash (182.5 ng) and Renilla control (0.5 ng) were transfected into cells by using Lipofectamine (Invitrogen, Carlsbad, CA). After 24 h, cells were lysed with the reporter lysis buffer (Promega, Madison, WI). Renilla and firefly luciferase activities were

measured by using *Renilla* luciferase assay and luciferase assay (Promega, Madison, WI). Each experiment was repeated at least three times in duplicate.

Statistical analysis

The results are expressed as mean \pm SEM. Statistical analysis involved using GraphPad Prism 9.0 for Windows (GraphPad Software, San Diego, CA, www.graphpad.com). All experiments were performed at least in triplicate. Two-way analysis of variance or Student *t* test was used for statistical analysis. $P < 0.05$ was considered statistically significant.

Supplementary Material

Supplementary Material is available at HMG online.

Acknowledgements

We thank the patients for giving their consent to take part in our study. We acknowledge Dr Agnes Ostertag for help with statistical analysis and Laura Smales (BioMedEditing, Toronto, Canada) for editing the manuscript.

Conflict of Interest statement. The authors declare that they have no conflict of interest in relation to the work.

Funding

European Union's Horizon 2020 research and innovation program under the Marie Skłodowska-Curie (grant agreement no. 766347). C.C.S. and R.R. received a fellowship from this grant. M.M. is a 'Maître de Recherche' at the 'Fonds National pour la Recherche Scientifique (FNRS)'.

References

- Slemenda, C.W., Turner, C.H., Peacock, M., Christian, J.C., Sorbel, J., Hui, S.L. and Johnston, C.C. (1996) The genetics of proximal femur geometry, distribution of bone mass and bone mineral density. *Osteoporos. Int.*, **6**, 178–182.
- Guéguen, R., Jouanny, P., Guillemin, F., Kuntz, C., Pourel, J. and Siest, G. (1995) Segregation analysis and variance components analysis of bone mineral density in healthy families. *J. Bone Miner. Res.*, **10**, 2017–2022.
- Koromani, F., Trajanoska, K., Rivadeneira, F. and Oei, L. (2019) Recent advances in the genetics of fractures in osteoporosis. *Front. Endocrinol.*, **10**, 337. <https://doi.org/10.3389/fendo.2019.00337>.
- Gregson, C.L., Newell, F., Leo, P.J., Clark, G.R., Paternoster, L., Marshall, M., Forgetta, V., Morris, J.A., Ge, B., Bao, X. et al. (2018) Genome-wide association study of extreme high bone mass: contribution of common genetic variation to extreme BMD phenotypes and potential novel BMD-associated genes. *Bone*, **114**, 62–71.
- Morris, J.A., Kemp, J.P., Youlten, S.E., Laurent, L., Logan, J.G., Chai, R.C., Vulpesu, N.A., Forgetta, V., Kleinman, A., Mohanty, S.T. et al. (2019) An atlas of genetic influences on osteoporosis in humans and mice. *Nat. Genet.*, **51**, 258–266.
- Forgetta, V., Keller-Baruch, J., Forest, M., Durand, A., Bhatnagar, S., Kemp, J.P., Nethander, M., Evans, D., Morris, J.A., Kiel, D.P. et al. (2020) Development of a polygenic risk score to improve screening for fracture risk: a genetic risk prediction study. *PLoS Med.*, **17**, e1003152. <https://doi.org/10.1371/journal.pmed.1003152>.
- Collet, C., Ostertag, A., Ricquebourg, M., Delecourt, M., Tueur, G., Isidor, B., Guillot, P., Schaefer, E., Javier, R.M., Funck-Brentano, T. et al. (2017) Primary osteoporosis in young adults: genetic basis and identification of novel variants in causal genes. *JBMR Plus*, **2**, 12–21.
- Mäkitie, R.E., Kämpe, A., Costantini, A., Alm, J.J., Magnusson, P. and Mäkitie, O. (2020) Biomarkers in WNT1 and PLS3 osteoporosis: altered concentrations of DKK1 and FGF23. *J. Bone Miner. Res.*, **35**, 901–912.
- Hartikka, H., Mäkitie, O., Männikkö, M., Doria, A.S., Daneman, A., Cole, W.G., Ala-Kokko, L. and Sochett, E.B. (2005) Heterozygous mutations in the LDL receptor-related protein 5 (LRP5) gene are associated with primary osteoporosis in children. *J. Bone Miner. Res.*, **20**, 783–789.
- Korvala, J., Löjja, M., Mäkitie, O., Sochett, E., Jüppner, H., Schnabel, D., Mora, S., Cole, W.G., Ala-Kokko, L. and Männikkö, M. (2012) Rare variations in WNT3A and DKK1 may predispose carriers to primary osteoporosis. *Eur. J. Med. Genet.*, **55**, 515–519.
- Luther, J., Yorgan, T.A., Rolvien, T., Ulsamer, L., Koehne, T., Liao, N., Keller, D., Vollersen, N., Teufel, S., Neven, M. et al. (2018) Wnt1 is an Lrp5-independent bone-anabolic Wnt ligand. *Sci. Transl. Med.*, **10**, eaau7137. <https://doi.org/10.1126/scitranslmed.aau7137>.
- Stürznickel, J., Rolvien, T., Delsmann, A., Butscheidt, S., Barvenčik, F., Mundlos, S., Schinke, T., Kornak, U., Amling, M. and Oheim, R. (2021) Clinical phenotype and relevance of LRP5 and LRP6 variants in patients with early-onset osteoporosis (EOOP). *J. Bone Miner. Res.*, **36**, 271–282.
- Baron, R. and Kneissel, M. (2013) WNT signaling in bone homeostasis and disease: from human mutations to treatments. *Nat. Med.*, **19**, 179–192.
- Huybrechts, Y., Mortier, G., Boudin, E. and Van Hul, W. (2020) WNT Signaling and bone: lessons from skeletal dysplasias and disorders. *Front. Endocrinol.*, **11**, 165. <https://doi.org/10.3389/fendo.2020.00165>.
- Krishnan, V., Bryant, H.U. and Macdougald, O.A. (2006) Regulation of bone mass by Wnt signaling. *J. Clin. Invest.*, **116**, 1202–1209.
- Kubota, T., Michigami, T. and Ozono, K. (2009) Wnt signaling in bone metabolism. *J. Bone Miner. Metab.*, **27**, 265–271.
- Maeda, K., Kobayashi, Y., Udagawa, N., Uehara, S., Ishihara, A., Mizoguchi, T., Kikuchi, Y., Takada, I., Kato, S., Kani, S. et al. (2012) Wnt5a-Ror2 signaling between osteoblast-lineage cells and osteoclast precursors enhances osteoclastogenesis. *Nat. Med.*, **18**, 405–412.
- Albers, J., Schulze, J., Beil, F.T., Gebauer, M., Baranowsky, A., Keller, J., Marshall, R.P., Wintges, K., Friedrich, F.W., Priemel, M. et al. (2011) Control of bone formation by the serpentine receptor Frizzled-9. *J. Cell Biol.*, **192**, 1057–1072.
- Zhang, Z., Rankin, S.A. and Zorn, A.M. (2013) Different thresholds of Wnt-frizzled 7 signaling coordinate proliferation, morphogenesis and fate of endoderm progenitor cells. *Dev. Biol.*, **378**, 1–12.
- Häusler, K.D., Horwood, N.J., Chuman, Y., Fisher, J.L., Ellis, J., Martin, T.J., Rubin, J.S. and Gillespie, M.T. (2004) Secreted frizzled-related protein-1 inhibits RANKL-dependent osteoclast formation. *J. Bone Miner. Res.*, **19**, 1873–1881.
- de Lau, W., Peng, W.C., Gros, P. and Clevers, H. (2014) The R-spondin/Lgr5/Rnf43 module: regulator of Wnt signal strength. *Genes Dev.*, **28**, 305–316.

22. Miller, J.R. (2002) The Wnts. *Genome Biol.*, **3**, REVIEWS3001. <https://doi.org/10.1186/gb-2001-3-1-reviews3001>.
23. Caetano da Silva, C., Ricquebourg, M., Orcel, P., Fabre, S., Funck-Brentano, T., Cohen-Solal, M. and Collet, C. (2021) More severe phenotype of early-onset osteoporosis associated with recessive form of LRP5 and combination with DKK1 or WNT3A. *Mol. Genet. Genomic Med.*, **9**, e1681. <https://doi.org/10.1002/mgg3.1681>.
24. Turin, C.G., Joeng, K.S., Kallish, S., Raper, A., Asher, S., Campeau, P.M., Khan, A.N. and Al Mukaddam, M. (2021) Heterozygous variant in WNT1 gene in two brothers with early onset osteoporosis. *Bone Rep.*, **15**, 101118. <https://doi.org/10.1016/j.bonr.2021.101118>.
25. Rocha-Braz, M., França, M.M., Fernandes, A.M., Lerario, A.M., Zanardo, E.A., de Santana, L.S., Kulikowski, L.D., Martin, R.M., Mendonca, B.B. and Ferraz-de-Souza, B. (2020) Comprehensive genetic analysis of 128 candidate genes in a cohort with idiopathic, severe, or familial osteoporosis. *JES*, **4**, 1–13.
26. Mäkitie, O. and Zillikens, M.C. (2021) Early-onset osteoporosis. *Calcif. Tissue Int.* <https://doi.org/10.1007/s00223-021-00885-6>.
27. Uysal-Onganer, P. and Kypta, R.M. (2012) Wnt11 in 2011 – the regulation and function of a non-canonical Wnt. *Acta Physiol.*, **204**, 52–64.
28. Boyan, B.D., Olivares-Navarrete, R., Berger, M.B., Hyzy, S.L. and Schwartz, Z. (2018) Role of Wnt11 during osteogenic differentiation of human mesenchymal stem cells on microstructured titanium surfaces. *Sci. Rep.*, **8**, 8588. <https://doi.org/10.1038/s41598-018-26901-8>.
29. Friedman, M.S., Oyserman, S.M. and Hankenson, K.D. (2009) Wnt11 promotes osteoblast maturation and mineralization through R-spondin 2. *J. Biol. Chem.*, **284**, 14117–14125.
30. Lako, M., Strachan, T., Bullen, P., Wilson, D.I., Robson, S.C. and Lindsay, S. (1998) Isolation, characterisation and embryonic expression of WNT11, a gene which maps to 11q13.5 and has possible roles in the development of skeleton, kidney and lung. *Gene*, **219**, 101–110.
31. Richards, S., Aziz, N., Bale, S., Bick, D., Das, S., Gastier-Foster, J., Grody, W.W., Hegde, M., Lyon, E., Spector, E. et al. (2015) Standards and guidelines for the interpretation of sequence variants: a joint consensus recommendation of the American College of Medical Genetics and Genomics and the Association for Molecular Pathology. *Genet. Med.*, **17**, 405–424.
32. Touma, M., Kang, X., Gao, F., Zhao, Y., Cass, A.A., Biniwale, R., Xiao, X., Eghbali, M., Coppola, G., Reemtsen, B. and Wang, Y. (2017) Wnt11 regulates cardiac chamber development and disease during perinatal maturation. *JCI Insight*, **2**, e94904. <https://doi.org/10.1172/jci.insight.94904>.
33. Sinha, T., Lin, L., Li, D., Davis, J., Evans, S., Wynshaw-Boris, A. and Wang, J. (2015) Mapping the dynamic expression of Wnt11 and the lineage contribution of Wnt11-expressing cells during early mouse development. *Dev. Biol.*, **398**, 177–192.
34. Garriock, R.J., D'Agostino, S.L., Pilcher, K.C. and Krieg, P.A. (2005) Wnt11-R, a protein closely related to mammalian Wnt11, is required for heart morphogenesis in *Xenopus*. *Dev. Biol.*, **279**, 179–192. <https://doi.org/10.1016/j.ydbio.2004.12.013> Erratum in: *Dev. Biol.* 2008 Oct **322**, 235.
35. Heisenberg, C.P., Tada, M., Rauch, G.J., Saúde, L., Concha, M.L., Geisler, R., Stemple, D.L., Smith, J.C. and Wilson, S.W. (2000) Silberblick/Wnt11 mediates convergent extension movements during zebrafish gastrulation. *Nature*, **405**, 76–81.
36. Heisenberg, C.P. and Nüsslein-Volhard, C. (1997) The function of silberblick in the positioning of the eye anlage in the zebrafish embryo. *Dev. Biol.*, **184**, 85–94.
37. Laine, C.M., Joeng, K.S., Campeau, P.M., Kiviranta, R., Tarkkonen, K., Grover, M., Lu, J.T., Pekkinen, M., Wessman, M., Heino, T.J. et al. (2013) WNT1 mutations in early-onset osteoporosis and osteogenesis imperfecta. *N. Engl. J. Med.*, **368**, 1809–1816.
38. Zhu, J.H., Liao, Y.P., Li, F.S., Hu, Y., Li, Q., Ma, Y., Wang, H., Zhou, Y., He, B.C. and Su, Y.X. (2018) Wnt11 promotes BMP9-induced osteogenic differentiation through BMPs/Smads and p38 MAPK in mesenchymal stem cells. *J. Cell. Biochem.*, **119**, 9462–9473.
39. Mori, H., Yao, Y., Learman, B.S., Kurozumi, K., Ishida, J., Ramakrishnan, S.K., Overmyer, K.A., Xue, X., Cawthorn, W.P., Reid, M.A. et al. (2016) Induction of WNT11 by hypoxia and hypoxia-inducible factor-1 α regulates cell proliferation, migration and invasion. *Sci. Rep.*, **6**, 21520. <https://doi.org/10.1038/srep21520>.
40. Tenjin, Y., Kudoh, S., Kubota, S., Yamada, T., Matsuo, A., Sato, Y., Ichimura, T., Kohroggi, H., Sashida, G., Sakagami, T. and Ito, T. (2019) Ascl1-induced Wnt11 regulates neuroendocrine differentiation, cell proliferation, and E-cadherin expression in small-cell lung cancer and Wnt11 regulates small-cell lung cancer biology. *Lab. Invest.*, **99**, 1622–1635.
41. Wilkesmann, S., Fellenberg, J., Nawaz, Q., Reible, B., Moghadam, A., Boccaccini, A.R. and Westhauser, F. (2020) Primary osteoblasts, osteoblast precursor cells or osteoblast-like cell lines: which human cell types are (most) suitable for characterizing 45S5-bioactive glass? *J. Biomed. Mater. Res. A*, **108**, 663–674.
42. Zhou, Y., Lin, J., Shao, J., Zuo, Q., Wang, S., Wolff, A., Nguyen, D.T., Rintoul, L., Du, Z., Gu, Y. et al. (2019) Aberrant activation of Wnt signaling pathway altered osteocyte mineralization. *Bone*, **127**, 324–333.
43. Maye, P., Zheng, J., Li, L. and Wu, D. (2004) Multiple mechanisms for Wnt11-mediated repression of the canonical Wnt signaling pathway. *J. Biol. Chem.*, **279**, 24659–24665.
44. Bisson, J.A., Mills, B., Paul Helt, J.C., Zwaka, T.P. and Cohen, E.D. (2015) Wnt5a and Wnt11 inhibit the canonical Wnt pathway and promote cardiac progenitor development via the caspase-dependent degradation of AKT. *Dev. Biol.*, **398**, 80–96.
45. van Amerongen, R., Fuerer, C., Mizutani, M. and Nusse, R. (2012) Wnt5a can both activate and repress Wnt/ β -catenin signaling during mouse embryonic development. *Dev. Biol.*, **369**, 101–114.
46. Qin, L., Yin, Y.T., Zheng, F.J., Peng, L.X., Yang, C.F., Bao, Y.N., Liang, Y.Y., Li, X.J., Xiang, Y.Q., Sun, R. et al. (2015) WNT5A promotes stemness characteristics in nasopharyngeal carcinoma cells leading to metastasis and tumorigenesis. *Oncotarget*, **6**, 10239–10252.
47. Kumawat, K. and Gosens, R. (2016) WNT-5A: signaling and functions in health and disease. *Cell. Mol. Life Sci.*, **73**, 567–587.
48. Jho, E.H., Zhang, T., Domon, C., Joo, C.K., Freund, J.N. and Costantini, F. (2002) Wnt/beta-catenin/Tcf signaling induces the transcription of Axin2, a negative regulator of the signaling pathway. *Mol. Cell Biol.*, **22**, 1172–1183.
49. Movérare-Skrtic, S., Henning, P., Liu, X., Nagano, K., Saito, H., Börjesson, A.E., Sjögren, K., Windahl, S.H., Farman, H., Kindlund, B. et al. (2014) Osteoblast-derived WNT16 represses osteoclastogenesis and prevents cortical bone fragility fractures. *Nat. Med.*, **20**, 1279–1288.
50. Glinka, A., Dolde, C., Kirsch, N., Huang, Y.L., Kazanskaya, O., Ingelfinger, D., Boutros, M., Cruciat, C.M. and Niehrs, C. (2011) LGR4 and LGR5 are R-spondin receptors mediating Wnt/ β -catenin and Wnt/PCP signalling. *EMBO Rep.*, **12**, 1055–1061.
51. de Lau, W., Barker, N., Low, T.Y., Koo, B.K., Li, V.S., Teunissen, H., Kujala, P., Haegerbarth, A., Peters, P.J., van de Wetering, M. et al. (2011) Lgr5 homologues associate with Wnt receptors and mediate R-spondin signalling. *Nature*, **476**, 293–297.
52. Gong, X., Carmon, K.S., Lin, Q., Thomas, A., Yi, J. and Liu, Q. (2012) LGR6 is a high affinity receptor of R-spondins and potentially

- functions as a tumor suppressor. *PLoS One*, **7**, e37137. <https://doi.org/10.1371/journal.pone.0037137>.
53. Knight, M.N., Karuppaiah, K., Lowe, M., Mohanty, S., Zondervan, R.L., Bell, S., Ahn, J. and Hankenson, K.D. (2018) R-spondin-2 is a Wnt agonist that regulates osteoblast activity and bone mass. *Bone Res.*, **6**, 24. <https://doi.org/10.1038/s41413-018-0026-7>.
 54. Jin, Y.R. and Yoon, J.K. (2012) The R-spondin family of proteins: emerging regulators of WNT signaling. *Int. J. Biochem. Cell Biol.*, **44**, 2278–2287.
 55. Martineau, X., Abed, É., Martel-Pelletier, J., Pelletier, J.P. and Lajeunesse, D. (2017) Alteration of Wnt5a expression and of the non-canonical Wnt/PCP and Wnt/PKC-Ca²⁺ pathways in human osteoarthritis osteoblasts. *PLoS One*, **12**, e0180711. <https://doi.org/10.1371/journal.pone.0180711>.
 56. Manousaki, D., Rauch, F., Chabot, G., Dubois, J., Fiscoletti, M. and Alos, N. (2016) Pediatric data for dual X-ray absorptiometric measures of normal lumbar bone mineral density in children under 5 years of age using the lunar prodigy densitometer. *J. Musculoskelet. Neuronal Interact.*, **16**, 247–255.
 57. Shpaer, E.G., Robinson, M., Yee, D., Candlin, J.D., Mines, R. and Hunkapiller, T. (1996) Sensitivity and selectivity in protein similarity searches: a comparison of Smith-waterman in hardware to BLAST and FASTA. *Genomics*, **38**, 179–191.
 58. Li, H. and Durbin, R. (2009) Fast and accurate short read alignment with burrows-wheeler transform. *Bioinformatics*, **25**, 1754–1760.
 59. Livak, K.J. and Schmittgen, T.D. (2001) Analysis of relative gene expression data using real-time quantitative PCR and the 2– $\Delta\Delta$ CT method. *Methods*, **25**, 402–408.
 60. Zhang, W., Zhuang, Y., Zhang, Y., Yang, X., Zhang, H., Wang, G., Yin, W., Wang, R., Zhang, Z. and Xiao, W. (2017) Uev1A facilitates osteosarcoma differentiation by promoting Smurf1-mediated Smad1 ubiquitination and degradation. *Cell Death Dis.*, **8**, e2974. <https://doi.org/10.1038/cddis.2017.366>.